This full text paper was peer reviewed at the direction of IEEE Communications Society subject matter experts for publication in the IEEE Globecom 2010 proceedings.

Surface Based Underwater Communications

Lloyd Emokpae and Mohamed Younis
Department of Computer Science and Electrical Engineering
University of Maryland Baltimore County
Baltimore, MD 21250
{lemokp1,younis}@cs.umbc.edu

***Abstract*—** In an underwater environment signal propagation for the acoustic channel is subject to major multipath effect. Therefore, most underwater communication schemes require that the position of the transmitter or receiver is fixed while using directional antennas in order to ensure high signal-to-noise ratio. However, such a requirement hinders node discovery and ad-hoc formation of underwater networks and restraints communication between autonomous underwater vehicles (AUVs) where node locations change over time. This paper proposes a novel approach to underwater communications by relying on the water surface to establish communication links. The proposed surface-based reflection (SBR) model works by requiring the transmitting node to direct its energy towards the water surface. The receiver then applies homomorphic deconvolution techniques to determine the channels impulse response used in obtaining the reflected signal. The receiver is then able to determine the location of the transmitter by triangulating the transmitted and reflected signals with respect to the water surface. Simulation experiments are provided to validate the SBR approach.

I. INTRODUCTION

Over the years underwater communications have found applications in oceanographic data collection, environmental monitoring, assisted navigation, and tactical surveillance [1]. In addition, recent years have witnessed an increase in applications of underwater acoustic sensor networks (UW-ASNs). UW-ASNs consist of stationary and mobile sensors that form a network in an ad-hoc manner and cooperatively work together to perform data acquisition over a specified area [2]. Furthermore, autonomous underwater vehicles (AUVs) are finding applications in search-and-rescue and coastal patrol. AUVs in these applications cooperate in task execution and thus need to establish and sustain communication links in order to ensure uninterruptible interactions [3]. This requires adapting to environmental changes and being able to detect communication holes due to external noise in the communication channel.

Underwater communications rely on acoustical channels instead of radio channels for long range communications since radio waves tend to get absorbed by the water medium. The water medium has an inhomogeneous property that is composed of water layers of different densities, salinity, and temperature which vary with depth. In an acoustic channel all of these properties affect the sound speed profile which changes with depth as shown in Figure 1, where the surface layer is mainly affected by the seasonal temperature changes and the thermocline layer is mainly due to the pressure effect which causes the water temperature to rapidly drop. In a shallow water environment acoustic waves tend to take multiple paths before arriving at the receiver with combinations of reflections from the surface and the bottom. To mitigate the effect of the multipath signal propagation, directional transmission schemes have been adapted for underwater communications [1][4][5][6]. These schemes require that the transmitter direct the acoustic antenna towards the known direction of the receiver.

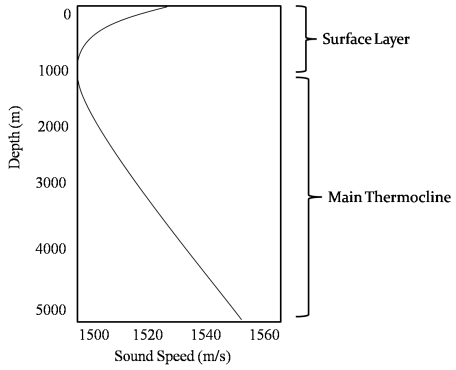

Figure 1: Pacific environment sound speed profile [7]. There are two main layers namely the surface layer and the main thermocline.

Therefore, node mobility poses a challenge for directional communication among nodes. In fact, even the location of non-mobile node tends to change over time due drift and water current. Generally, in an environment where the location of the source and the destination might be unknown it is not possible for the receiver to discover the location of the transmitter due to the multipath effect of the channel. Such type of communication will require that the transmitter spread the signal using an omnidirectional scheme to properly communicate with the receiver [5], which would require a high transmission power. On the other hand, establishing a relative topology using localization techniques, e.g., the received-signal-strength (RSS), the time-of-arrival (TOA) or the angle-of-arrival (AOA), requires the consideration of measurements made by nodes in the vicinity, which would not be possible given the lack of communication links among neighbors. In addition, these measurements (especially TOA) can have errors due to the multipath signals arriving sooner than expected, and due to the attenuated line of sight signals which decreases the accuracy of the TOA estimation [8].

To overcome the limitations of present systems, this paper

proposes a surface-based reflection (SBR) scheme that uses the reflections from the water surface to establish communication links. The receiver only accepts signals that are reflected at the surface by checking the RSS and comparing it to the calculated reflection coefficients. This is done by applying a homomorphic deconvolution process to the received signal to obtain the impulse response (IR) of the acoustic channel containing the RSS information. Advantages of the SBR method include source signal tracking avoidance, node localization, and network link extensions. Simulation experiments are provided to validate the SBR approach.

The paper is organized as follows. In section II, we discuss related work in the literature. Section III goes over the system model and section IV describes the proposed SBR method in detail. The approach is evaluated in section V. Section VI concludes the paper.

II. Related Work

A. Underwater Channel Multipath Effects

In shallow water communications the effects of the multipath channel is often pronounced. Hence, the receiver typically applies matched filters to the estimated channel IR before recovering the transmitted signal in order to counter the effects of the multipath [5][9]. This type of method is typically termed *blind equalization*, since the main goal is to extract the transmitted signal from the statistics of the received signal with the estimated channels IR. The channel IR is estimated by using the receiver-transmitter geometry and the physical properties of the water medium. However, this method is limited by the receiver's inability to determine the transmitter's location due to the multipath effect of the channel the receiver. This method also assumes a fixed receiver or transmitter which is not practical for communication between AUVs.

In [6], underwater channel estimation has been studied for communication between AUVs, where the movement of both the transmitter and the receiver is factored in the acoustic channel model. The effects of movement are captured as time variations in the delays and amplitude of the channels IR. These variations are mitigated by increasing the directivity of the transmission which also decreases the number of propagation paths. However, increasing the transmission directivity requires a foreknowledge of the location of the receiver which is not always possible.

B. Water Surface Effects

The effect of the water surface was studied in [10] [11], where the transmission line matrix (TLM) was used to model the shallow water acoustic channel in [10]. The water surface was used to determine the transmitters self-inducing echo in [11]. A self-inducing echo will cause the channel contender (in a channel access scheme) to hear its own transmission reflected from the water surface and interpret that as another node which causes the contender to back-off and never be able to transmit data. A self-reflection tone learning (SRTL) algorithm was implemented where the transmitter detects its self inducing echo caused by the water surface. This is different from the proposed SBR model since SRTL the algorithm works at the MAC layer and allows the reflections to be present in the physical layer. This approach is also limited by its dependency on the Bayesian conditional probability of the echo being induced by the transmitter.

C. Node localization

There has been significant research in indoor radio localization that estimates the channel's IR to determine the RSS. For example, Hashemi [12] used the measured IR to characterize the indoor radio propagation in two office buildings where signal reflections of the building where considered random and uncorrelated to the signal's attenuation. Hence the measurement of the RSS in [12] was mainly dependent on the recovery of the direct path signal, which may not arrive at a mobile receiver. Meanwhile, the focus of [2] was on the TOA measurements where matched filters were used to remove the unwanted noise in the underwater channel. This approach improves the estimation of the channel's IR to obtain both the RSS and the TOA. However, this approach is dependent on the direct path which is not practical for communication between AUVs. The proposed SBR model avoids such dependency by reflecting signals from the water surface, which allows for nodes to be mobile during localization.

III. System Model

The communication model considered in this paper is summarized in Figure 2. The transmitter block is described in the balance of this section. The receiver block is deduced in section IV. This paper acknowledges the need for a filter that removes the channel noise *n(t)* and assumes a filter design similar to [2]. It is assumed that the transmitter's position is encoded in the message *e(t)* before being sent to the receiver, this requires the transmitter to have an integrated inertial navigational system (INS) with an acoustical aid to determine its position as demonstrated in [13], The position of the transmitting node is composed of the latitude, longitude and depth. The INS in the transmitter will be initialized before being deployed in the water; the initial position estimates will be geographically referenced. After deployment, the INS will track its position relative to the reference location by using triaxial accelerometers; this will drift over time and can be corrected by using the TOAs measurements between connected transmitter-receiver pairs.

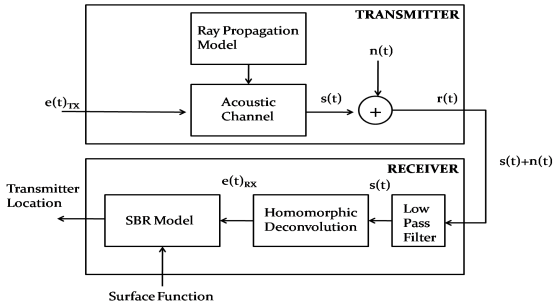

Figure 2: Block diagram description of the assumed transmitter and receiver models. The transmitter uses a ray propagation model to predict the channels IR.

A. Ray Propagation Model

The ray propagation model is a widely-accepted method for modeling signal propagation in shallow water [6][14][16]. According to Paul C. Etter [6] there are typically four basic types of eigenrays that are of interest as shown in Figure 3, namely: refracted-surface-reflected (RSR), refracted-bottom-reflected (RBR), refracted-surface-reflected-bottom-reflected (RSRBR), and the direct-path (DP).

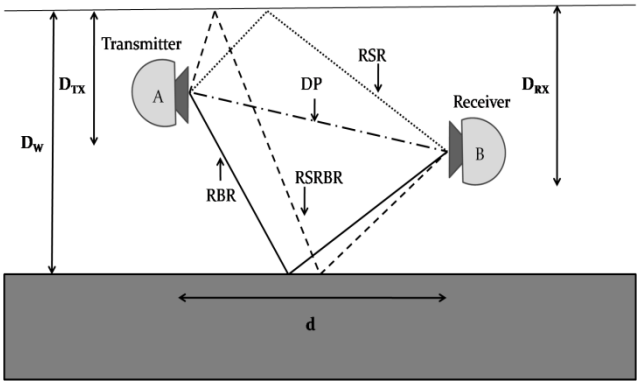

Figure 3: Illustrating the four eigenray types

Florian Schulz [5] went on to describe the length of each eigenray which is reflected at the surface first before being reflected *i* times during the entire propagation as:

$$r_i = \sqrt{(D_{TX} + a_i D_w + b_i D_{RX})^2 + d^2} \quad (1)$$

The geometrical descriptions of the transmitter and the receiver are illustrated in Figure 3. The coefficients for a_i and b_i are given in (2), (3), and (4).

$$a_1 = 0 \quad (2)$$

$$a_{i+1} = a_i + (1 + (-1)^{i+1}) \quad (3)$$

$$b_i = (-1)^{i+1} \quad (4)$$

B. Estimating the channels impulse response

A multipath channel acts like a delay line where each path is delayed according to the path's eigenray length. The baseband IR of the channel can be modeled as follows:

$$h(t) = \sum_{i=1}^{K} \beta_i \, \eth(t - \tau_i) \quad (5)$$

$$\tau_i = \frac{r_i}{c_w} \quad (6)$$

The values of β_i and τ_i correspond to the attenuation factor and the time delay respectively. The propagation delay τ_i is expressed in (6) is dependent on the eigenray length. The attenuation factor β_i is assumed to be the product of the reflection coefficients corresponding to the bounces along the i^{th} path with absorption loss coefficient along each path. The function $\eth(t)$ is the Dirac delta function. The transmitted signal $e(t)$ is convolved with the channel's IR $h(t)$ which is assumed to be stable and produces the noise free signal $s(t)$. The noisy signal $n(t)$ is assumed to be uncorrelated to the noise-free signal and could be model as a white noise. Finally, the received signal is simply expressed in (8).

$$s(t) = e(t) * h(t) \quad = \sum_{i=1}^{K} \beta_i \, e(t - \tau_i) \quad (7)$$

$$r(t) = s(t) + n(t) \quad (8)$$

IV. UNDERWATER SURFACE-BASED REFLECTION

A. Surface Reflection Model

Instead of relying on the direct path from the source to the receiver, we promote using the refracted-surface-reflected (RSR) eigenray as the communication link between the transmitter and the receiver. The laws of reflection tell us how to determine the reflected vector $\overrightarrow{r_B}$ if we know the surface function. The sampled transmitted signal e(t) can be represented as a vector in R^3 as described in (9). We note that the "*" operation represents the dot product operator and $\vec{n}$ is the normal vector that is normal to the water surface.

$$\overrightarrow{r_A} = r_{Ax}\hat{x} + r_{Ay}\hat{y} + r_{Az}\hat{z} \quad (9)$$

$$\overrightarrow{r_B} = \overrightarrow{r_A} - 2(\overrightarrow{r_A} * \vec{n})\vec{n} \quad (10)$$

$$\overrightarrow{r_{AB}} = \overrightarrow{r_A} - (\overrightarrow{r_A} * \vec{n})\vec{n} \quad (11)$$

This model requires that the receiver knows the surface function of the water surface which can vary with time as shown in Figure 4. We should also point out that in a real underwater environment the water surface will not be stationary, however due to the ratio of the fastest ocean wave (150 m/s) speed to the speed of sound (1500 m/s) both the receiver and the transmitter will perceive the wave as stationary upon signal reception at the receiver. This is illustrated in [10], where transmission line matrix (TLM) was used to show the effects of the water surface on the received signal. So for ease of analysis we can assume that the water surface in Figure 4 is stationary, note that the surface normal's are plotted along the surface function, since the surface normal's are changing we can expect the reflected vector to change, but we are only interested in the surface normal $\vec{n}$ at the intersection point (x_0, y_0, z_0). The surface normal $\vec{n}$ is the vector that is perpendicular to the tangent plane $p(x, y)$ that intersects the surface function at the point (x_0, y_0, z_0).

We could solve for the normal vector by picking out any three points (P_1, P_2, P_3) that lie on the tangent plane $p(x, y)$ and compute the cross product of their differences as shown:

$$\vec{n} = (P_1 - P_2) \times (P_1 - P_3)$$

If the water surface "S" has a surface equation in the form: $z = f(x, y)$, Where (x_0, y_0, z_0) is a point on S and f has a continuous first partial derivative, the equation to the tangent plane can be expressed as:

$$z = f_x(x_0, y_0)(x - x_0) + f_y(x_0, y_0)(y - y_0) + f(x_0, y_0)$$

$$p(x, y) = f_x(x_0, y_0)(x - x_0) + f_y(x_0, y_0)(y - y_0) + f(x_0, y_0) \quad (12)$$

If the partial derivatives f_x and f_y are not continuous but exist near the point (x_0, y_0) we can obtain an approximation to the partial derivatives and the tangent plane as:

$$f_x(x_0, y_0) = \lim_{h \to 0} \frac{f(x_0 + h, y_0) - f(x_0, y_0)}{h}$$

$$f_y(x_0, y_0) = \lim_{h \to 0} \frac{f(x_0, y_0 + h) - f(x_0, y_0)}{h}$$

$$p(x, y) \approx f_x(x_0, y_0)(x - x_0) + f_y(x_0, y_0)(y - y_0) + f(x_0, y_0)$$

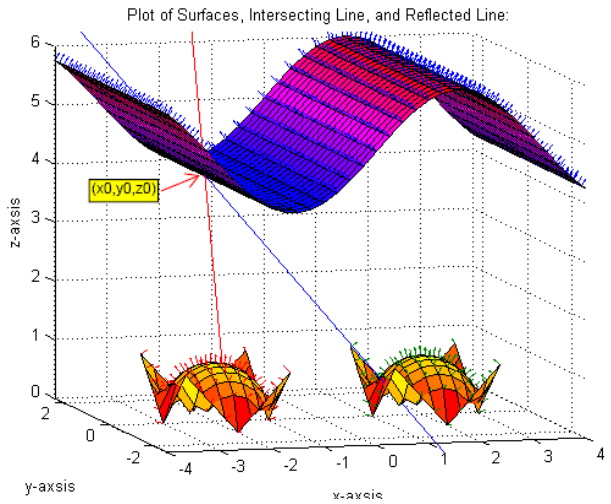

Figure 4: Plot of surface function with the transmitted and reflected vectors

From the tangent plane equation we can compute the normal vector which is used to determine the location of the transmitter as described in (11). This model assumes that the combination of both the transmitted and the reflected lines is the RSR eigenray, which is only valid if other eigenrays are filtered out at the receiver. The next section goes over the receiver's filter design so that it only accepts the RSR eigenray.

B. Multipath deconvolution for the surface reflection model

To recover the RSR eigenray we can apply a homomorphic deconvolution to the noise free received signal by using the methods in the cepstrum analysis described by Oppenheim & Shafer [15]. A homomorphic system has the properties whereby the convoluted input signals can be transformed into the logarithm of their z-transforms. Hence, we can derive the complex cepstrum of the noise-free received signal from the sampled noise free received signal s[n] by recalling the convolution property defined in (7):

$$s[n] = e[n] * h[n]$$

$$s[n] = s_c\left(n\frac{1}{f_s}\right) = s_c(nT_s)$$

So we can define the z-transforms of the discrete signal as follows:

$$S(z) = Z(s[n]) = E(z)H(z)$$

Hence we have:

$$\hat{S}(z) = \log[S(z)] = \log[E(z)] + \log[H(z)]$$

$$\hat{S}(z) = \hat{E}(z) + \hat{H}(z)$$

$$\hat{s}[n] = D_*[e[n] * h[n]] = \hat{e}[n] + \hat{h}[n] \quad (13)$$

The expression (13) is termed the complex cepstrum of the discrete signal $s[n]$ and requires both $\hat{e}[n]$ and $\hat{h}[n]$ to be stable, meaning that their region of convergence (ROC) must contain the unit circle.

If both $\hat{e}[n]$ and $\hat{h}[n]$ are in different quefrency ranges (measurement of time in samples), a linear filter can be applied to the complex cepstrum of the noise free received signal $\hat{s}[n]$ to recover both the channel's IR $h[n]$ and the transmitted signal $e[n]$, the homomorphic deconvolution processes for $h[n]$ and $e[n]$ are shown in Figure 5.

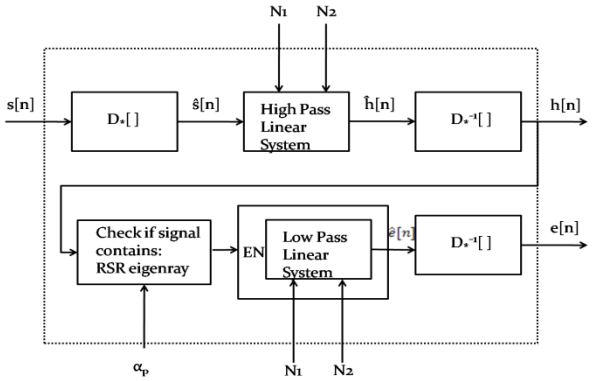

Figure 5: The deconvolution process uses the noise-free received signal as input. The function block $\boldsymbol{D}_*[]$ obtains the complex cepstrum of the signal as described in (13).

The IR deconvolution process requires that the parameters N_1 and N_2 be defined, their expressions are given in (14) and (15), the filter is implemented using DFTs of length N = 4096. The sound speed in the water layer c_w can be obtained from the sound speed profile in Figure 1. The filter also requires that an optimal distance between the transmitter and the receiver to be defined as the maximum distance required for ensuring that the received signal is within the desired decibel range. The time response of the high pass system is shown in Figure 6, a similar response can be obtained for the low pass system.

$$N_1 = \frac{d}{c_w} * \frac{1}{T_s} \quad (14)$$

$$N_2 = \frac{N}{2} \quad (15)$$

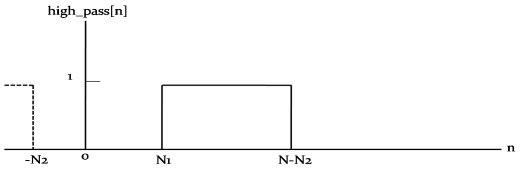

Figure 6: Time response for the high pass system

All eigenrays except the RSR eigenray will be reflected in the water bottom floor (i.e. rocks, soil) or in the bottom of the surface layer as shown in Figure 1 with an attenuation factor of α_p which will affect the magnitude of the IR.

V. Approach Evaluation

The deconvolution process required to recover the RSR signal is validated through simulation. This section describes the experiments setup and analyzes the simulation results.

A. Experiments Setup

The channel's IR is simulated in MATLAB by using the parameters in Table 1. Basically, we study the effect of the various parameters on the effectiveness of the proposed SBR approach. Every row in Table 1 lists the values used when varying the parameter in the shaded cell. Table 2 provides the values used when varying a certain parameter in the corresponding column. The transmitted signal is obtained from

a 10 KHz sampled speech file from [17]. The transmitted signal can also be an encoded stream that contains the transmitter's location but the receiver might need to use an all-pass filter to convert the unstable system into a stable one required for cepstral analysis.

DT_x (m)	DR_x (m)	D_w (m)	c_b (m/s)	p_b (kg/ m^3)	α_p (dB/km)	d (m)
DT_x	10	30	1510	999.95	0.25	10
15	DR_x	30	1510	999.95	0.25	10
15	10	30	1510	999.95	0.25	10
15	10	D_w	c_b	p_b	0.25	10
15	10	30	1510	999.95	α_p	10
15	10	30	1510	999.95	0.25	d

Table 1: The simulation parameters for the channel's IR, the speed of sound in the water layer c_w is assumed to be 1520 m/s for all runs, while 10 total eigenrays are simulated in all cases. The parameters in the shaded cells are varied according to the corresponding column in Table 2.

run	DT_x (m)	DR_x (m)	D_w (m)	c_b (m/s)	p_b (kg/ m^3)	α_p (dB/km)	d (m)
1	25	20	30	1510	999.95	0.15	10
2	23	18	32	1509	1000	0.20	11
3	21	16	34	1508	1000.05	0.25	12
4	19	14	36	1507	1000.10	0.30	13
5	17	12	38	1506	1000.15	0.35	14
6	15	10	40	1505	1000.20	0.40	15

Table 2: Values for the varied simulation parameters in Table1.

In the first two rows of Table 1 the depth of both the transmitter and the receiver decreases which simulates both the transmitter and the receiver moving closer to the water surface. We also modify the water depth which will affect the bottom layer sound speed and density. The cut-off values for the low/high pass filters (with $N = 4096$ and $d = 10$) can be calculated from equations (14) and (15). The sampling period T_s is taken to be 0.1ms. Hence, we have a total of 410 ms of received signal data with 4096 total samples.

B. Simulation Results

The simulated channel IR for the parameter values in the third row of Table 1 is the dark curve in Figure 7, the impulses corresponds to the arrival times of the multipath signal. The first TOA corresponds to the RSR eigenray which is attenuated to about 0.28, all other impulses corresponds to eigenrays that are reflected by the water bottom and are attenuated even more as shown. The noise free transmitted signal is depicted in Figure 8. Examining the plot indicates that from the 177th sample (arrival of the RSR eigenray impulse) to about the 440th sample the noise-free received signal is identical to the transmitted signal, after which we start to see the effect of the other arriving eigenrays on the received signal. The recovered channel IR and the RSR signal are shown in Figure 7. From the plot we see that the recovered channel IR resembles the simulated channel IR for filter parameters of N_1=66 and N_2=2048. The amplitude fluctuations from the 128th sample to about the 300th sample are due to the parameters used in the filter design. It is important to note that this can be controlled by tuning the values of N_1 and N_2. Figure 7confirms the effectiveness of the homomorphic deconvolution process used by the receiver to recover the RSR signal in an underwater multipath environment.

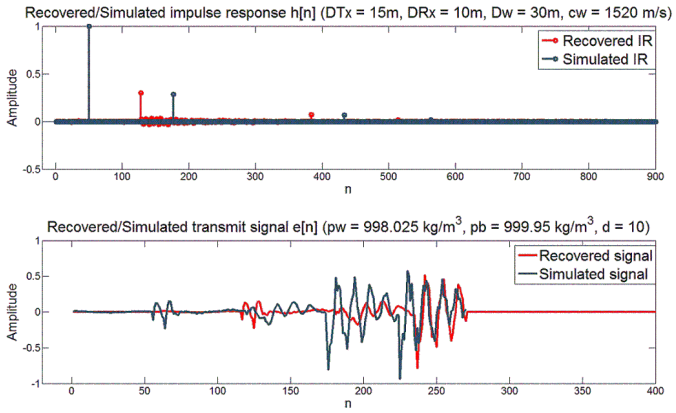

Figure 7: Plot showing the simulated and recovered channel IR with the RSR speech signal for the non-varying simulation parameters.

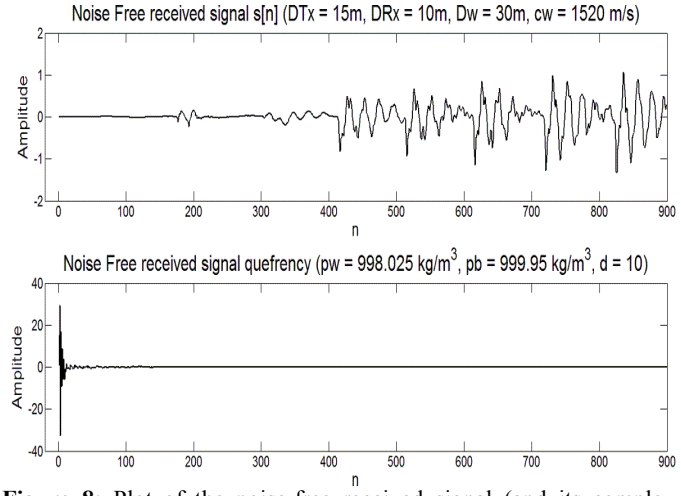

Figure 8: Plot of the noise-free received signal (and its complex cepstrum) that shows the effects of the multipath channel on the received signal.

The results in Figure 9 show that the transmitter-receiver depths greatly affect the RSR impulse delay. If we hold the other parameters constant and vary the transmitter depth DT_X , we notice that for a transmitter depth of 25m (run #1) the RSR impulse delay is about 24 ms, as the transmitter moves closer to the water surface the RSR eigenray length becomes shorter which reduces the RSR impulse delay. The same effect holds true for the receiver DR_X which whose delay matches DT_X as depicted in Figure 9. On the other hand, varying the transmitter-receiver distance "d" has a minimal affect on the delay. Finally, the water depth "D_w" does not affect the delay, which is expected since the RSR eigenray will not interact with the water bottom. Despite the delay variation the recovery of the RSR signal (Figure 7) is not hindered by the mobility of the transmitter or receiver.

Analyzing the results in Figure 10 indicates that the speed of sound c_b greatly affects the RSR amplitude if either the

transmitter or the receiver is close to the water bottom. Hence the effect of the sound speed c_b on the RSR amplitude will be mitigated when both the transmitter and receiver are closer to the water surface or by increasing the transmit energy. The water bottom density "p_b", the water depth "D_w" and the transmitter-receiver distances "d" will have minimal effect on the RSR amplitude as shown. Varying both transmitter-receiver depths "DT_X" and "DR_X" will not affect the recovery of the RSR signal when α_p is held constant at 0.25.

Overall, the experiments demonstrate that for an accurate estimate of the bottom attenuation parameter α_p we can recover the RSR signal which is used to determine the location of the transmitter as shown in (11). The bottom attenuation parameter can be measured in a multilayer oceanic environment (Figure 1) or estimated from known seafloor materials, i.e., clay, sand, gravel, etc., in shallow water environments. The results confirm that the SBR approach performs as expected and suits underwater communications.

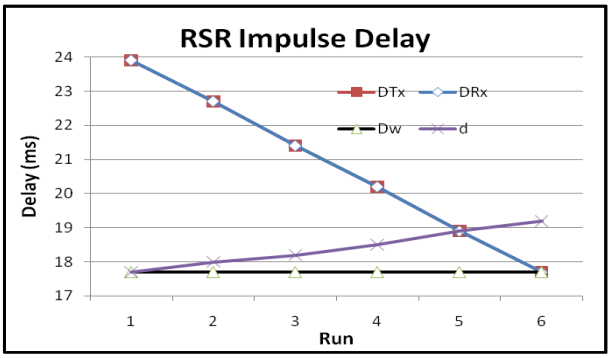

Figure 9: RSR Impulse delay shows the effects of varying the parameters according to Table 2

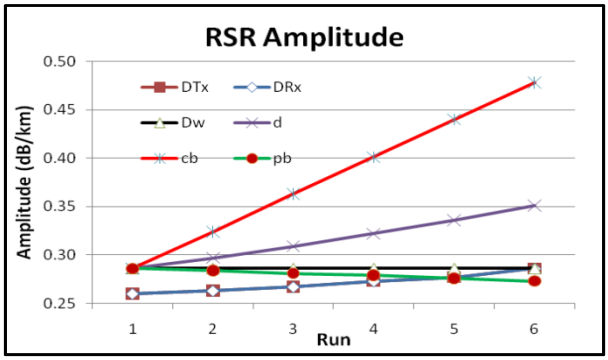

Figure 10: The effect on the RSR amplitude when varying the parameters in Table 2

VI. Conclusion

In this paper we have presented a novel approach to underwater communications by using the water surface to establish communication links. The channel's IR is affected by the transmitter-receiver depths and the oceanic environment, and hence the ray propagation model is used to simulate the noise-free received signal. The receiver applies homomorphic deconvolution techniques to determine the channel's IR used to recover the RSR signal. The SBR model computes the tangent plane to the stationary water surface to determine the normal vector at the point that the RSR signal intersects the water surface function and determines the location of the transmitting node.

The simulation experiments confirm the effectiveness of the homomorphic deconvolution process used to recover the RSR signal. The results also show that the transmitter-receiver depths will affect the recovery of the RSR signal due to the variation in the RSR arrival times. The transmitter-receiver depths will also affect the RSR amplitude when one of the nodes is close to the water bottom layer due to the decrease in compressional-wave speed, and hence the SBR model is very effective when both the transmitter and receiver are closer to the water surface. The SBR method can be further extended to consider both RSR and RBR links by considering signals that are reflected from the water bottom.

References

[1] M. Stojanovic, "Underwater Acoustic Communications," in *Encyclopedia of Electrical and Electronics Engineering*, Vol. 22, John G. Webster, John Wiley & Sons, pp. 688–698, 1999.

[2] I. F. Akyildiz, D. Pompili, and T. Melodia, "Underwater Acoustic Sensor Networks: Research Challenges," *Ad Hoc Networks*, Vol. 3, No. 3, pp. 257-279, March 2005.

[3] B.M. Howe, T. McGinnis, H. Kirkham, "Sensor networks for cabled ocean observatories," *Geophysical Research Abstracts*, Vol. 5, pp. 113-120, 2004.

[4] A. Jarrot, C. Ioana, and A. Quinquis, "Denoising Underwater Signals Propagating through Multi-path Channels," *Proc. IEEE/OES OCEANS`05 EUROPE Conf.*, Brest, France, Vol. 1, pp. 501-506, June 2005.

[5] F. Shulz, R. Weber, A. Waldhorst and J.F. Bohme, "Performance Enhancement of Blind Adaptive Equalizers Using Environmental Knowledge," *Proc. of the IEEE/OES OCEANS Conference*, Vol. 4, pp. 1793-1799, San Diego, CA,2003.

[6] A. Essebar, G. Loubet, F. Vial, "Underwater Acoustic Channel Simulations for Communication," *Proc. of the IEEE/OES OCEANS`94 Conference,* Vol. 3, pp. 495-500, 1994.

[7] M. B. Porter, "Acoustic Models and Sonar Systems," *IEEE Journal of Oceanic Engineering*, Vol. 18, No. 4, pp. 425-437, October 1993.

[8] G. Carter, "Coherence and Time Delay Estimation," *Proceedings of the IEEE*, Vol. 75, No. 2, pp. 236-255, 1993

[9] B.S. Sharif, J. Neasham, D. Thompson, O.R. Hinton, and A.E. Adams, "A blind multichannel combiner for long rage underwater communications," *Proc. of the IEEE International Conference on Acoustics, Speech and Signal Processing (ICASSP'97)*, Munich, Germany, April 1997.

[10] I.J.G. Scott and D. de Cogan, "Acoustic wave propagation in underwater shallow channel environments", *Proc. of the IEEE/OES OCEANS`07 EUROPE Conference,* pp. 1-6, 2007.

[11] A. A. Syed, "Understanding and Exploiting the Acoustic Propagation Delay in Underwater Sensor Networks," Ph.D. Dissertation Department of Computer Science, University of South Califonia, 2009.

[12] H. Hashemi, "The Indoor radio propagation channel," Proceedinsg of the IEEE, Vol. 81, No. 7, pp. 943-968, 1993.

[13] R. Marthiniussen, J.E. Faugstadmo and H.P. Jakobsen, "HAIN: an integrated acoustic positioning and inertial navigation", *Proc. of IEEE TECHNO-OCEAN '04*, Vol. 3, pp. 1620-1628, 2004.

[14] P. C. Etter, Underwater Acoustic Modeling, Principles, Techniques and Applications, 2nd edition, E & FN Spon, 1996.

[15] Oppenheim & Shafer, *Discrete-Time Signal Processing*, 3rd edition.

[16] F.B. Jensen, W.A. Kuperman, M.B. Porter, H. Schmidt, *Computational Ocean Acoustics*, Springer New York, 2nd edition.

[17] T.F. Quatieri, Discrete-Time Speech Signal Processing: Principles and Practices, Prentice Hall PTR, November 2001